Magneto-thermo-elastic response of exponentially graded piezoelectric hollow spheres

M.N.M. Allam[1], R. Tantawy[2] and A.M. Zenkour[3,4]*

[1]Department of Mathematics, Faculty of Science, Mansoura University, Mansoura 35516, Egypt
[2]Department of Mathematics, Faculty of Science, Damietta University, Damietta 34517, Egypt
[3]Department of Mathematics, Faculty of Science, King Abdulaziz University, Jeddah 21589, Saudi Arabia
[4]Department of Mathematics, Faculty of Science, Kafrelsheikh University, Kafrelsheikh 33516, Egypt

Abstract. This article presents a semi-analytical solution for an exponentially graded piezoelectric hollow sphere. The sphere interacts with electric displacement, elastic deformations, electric potentials, magneto-thermo-elasticity, and hygrothermal influences. The hollow sphere may be standing under both mechanical and electric potentials. Electro-magneto-elastic behavior of magnetic field vector can be described in the hollow sphere. All material, thermal and magnetic properties of hollow sphere are supposed to be graded in radial direction. A semi-analytical technique is improved to deduce all fields in which different boundary conditions for radial stress and electric potential are presented. Numerical examples for radial displacement, radial and hoop stresses, and electric potential are investigated. The influence of many parameters is studied. It is seen that the gradation of all material, thermal and magnetic properties has particular effectiveness in many applications of modern technology.

Keywords: exponentially graded material; semi-analytical technique; perturbation of magnetic field; hygrothermal effect; piezoelectric materials

1. Introduction

Different graded materials are inhomogeneous composite materials that varied smoothly and continuously as functions of position in thickness direction of structures. These materials are mainly organized to operate in hygrothermal environment. Recently, the interest to manufacture components with improved composition materials has been increased through their functionally gradation for an optimized design. The main application of functionally (FGMs) or exponentially (EGMs) graded materials increases in high temperature aerospace circumference. Ding *et al*. (2003) presented the spherically symmetric thermoelastic problem of a FG pyroelectric hollow sphere. Eslami *et al*. (2005) presented a general solution for the 1D steady-state thermal and mechanical stresses in FGM hollow thick spheres. Poultangari *et al*. (2008) obtained the solution for the 2D steady state thermal and mechanical stresses in a FGM hollow thick sphere. Kar and Kanoria (2009) presented a generalized thermoelastic FG orthotropic hollow sphere subjected to

---

thermal shock with three-phase-lag effect.

An extension to the FGMs is the functionally graded piezoelectric materials (FGPMs) (Guo *et al.* 2009, Ghobanpour Arani *et al.* 2012, Akbarzadeh and Chen, 2013, Jabbari *et al.* 2013). Dai and Fu (2005) presented an analytical method to obtain electromagnetoelastic transient behavior of piezoelectric spheres in constant magnetic field. Dai *et al.* (2007) studied analytical solution for piezoelectric response in FGP cylinder and sphere under mechanical loadings and electric excitation. Ootao and Tanigawa (2007) treated theoretically the transient thermo-piezo-electric response of FG sphere due to uniform heat supply. Chiroiu and Munteanu (2007) analyzed the free vibrations of a piezoceramic hollow sphere with radial polarization by using the cnoidal method and a genetic algorithm. Dai *et al.* (2008) discussed analytical investigations on electro-magneto-elastic response of FGP cylinder and sphere rested in constant magnetic field and undergo mechanical and electric loadings. Wang and Xu (2010) carried out the elastic analysis for FG, radially polarized piezoelectric spherical structure subjected to mechanical and electrical loads based on the 3D linear piezoelectric theory. Allam and Tantawy (2011) discussed analytically the interaction of electric potential and displacement, elastic deformation and thermoelasticity in FG hollow structures. Dai *et al.* (2012) investigated an analytical solution for time-dependent behaviors of a FGPM hollow sphere subjected to the coupling of multi-fields. Arefi and Nahas (2014) developed the nonlinear thermos-electro-elastic analysis of a thick spherical shell for the FGPMs. Allam *et al.* (2015) presented semi-analytical technique for FGP hollow spheres.

Many investigations concerning global responses of EG/FG elastic, piezoelectric, or viscoelastic structures in thermal or hygrothermal environments are made in the literature (Reddy and Chin, 1998, Reddy, 2000, Reddy and Cheng, 2001, Zenkour, 2005a, b, 2006, 2007, Zenkour *et al.* 2008, Ghorbanpour Arania *et al.* 2009, 2011, Loghman *et al.* 2011, Allam *et al.* 2017). Wang and Ding (2006) solved the transient responses of a magneto-electro-elastic hollow sphere subjected to spherically symmetric dynamic loads. Dai and Rao (2011) presented an analytical method to investigate electro-magneto-thermo-elastic responses of a FGPM hollow sphere placed in a uniform magnetic field, subjected to electric, thermal and mechanical loads. Dai *et al.* (2011) investigated the exact solution for the 1D steady-state magneto-thermo-elastic stresses and perturbation of magnetic field vector in FGM hollow spheres. Ootao and Ishihara (2012) investigated the theoretical analysis of a multilayered magneto-electro-thermo-elastic hollow sphere under unsteady and uniform surface heating. Chen *et al.* (2015) presented an analytical solution on the general static deformation of a spherically anisotropic and multilayered magneto-electro-elastic hollow sphere.

In this article, a semi-analytical technique for an EGP hollow sphere is presented. The hollow sphere interacts with electric potential, electric displacement, elastic deformations, magneto-thermo-elasticity, and hygrothermal influences. Different examples are investigated for EGP sphere is subjected to various types of pressures. The effect of many parameters and various boundary conditions on the field study of EGP hollow sphere are discussed.

2. Basic equations

Consider a hollow sphere, which has a perfect conductivity and placed in a constant magnetic field. Here, the spherical coordinates system (r, θ, φ) is used for any representative point and the EGP sphere is based upon rapid change in temperature $T(r)$, moisture concentration $C(r)$ and mechanical loads. In what follows the index i will represent r and θ while the index j will represent r, θ, and φ.

Here, the property variation $P(r)$ of all material properties in EGP sphere across the radial direction is supposed as

$$P(r) = p^a e^{\frac{k(r-a)}{b}}, \quad k = \frac{b}{b-a} \ln\left(\frac{p^b}{p^a}\right), \tag{1}$$

in which a and b denote inner and outer radii of hollow sphere, respectively, p^a represents the corresponding material property of the inner surface while p^b represents the corresponding material property of outer surface. We will present the basic equations of the EGP sphere for the axisymmetric plane strain assumption in the following relations:

The constitutive relations are (Sinha 1962, Raja *et al.* 2004, Dai and Wang 2005):

$$\begin{Bmatrix} \sigma_r \\ \sigma_\theta \end{Bmatrix} = \begin{bmatrix} c_{rr} & 2c_{r\theta} & e_{rr} \\ c_{r\theta} & c_{\theta\varphi} + c_{\theta\theta} & e_{r\theta} \end{bmatrix} \begin{Bmatrix} \dfrac{du}{dr} \\ \dfrac{u}{r} \\ \dfrac{d\psi}{dr} \end{Bmatrix} - \begin{Bmatrix} \lambda_r \\ \lambda_\theta \end{Bmatrix} T(r) - \begin{Bmatrix} \eta_r \\ \eta_\theta \end{Bmatrix} C(r), \tag{2}$$

and

$$D_r = e_{rr} \frac{du}{dr} + 2e_{r\theta} \frac{u}{r} - \varepsilon_{rr} \frac{d\psi}{dr} + p_{rr} T(r), \tag{3}$$

where $\sigma_i(r)$ denote stress components, $D_r(r)$ denotes electric displacement, $u(r)$ represents radial displacement, and $\psi(r)$ represents the electric potential. Also, c_{ij} denote the elastic coefficients, e_{ri} denote the piezoelectric parameters, ε_{rr} represent the dielectric parameter and p_{rr} represents the pyroelectric coefficient. In addition, η_i represent the moisture expansion coefficients while λ_i denote stress-temperature moduli which expressed in the forms

$$\begin{Bmatrix} \lambda_r \\ \lambda_\theta \end{Bmatrix} = \begin{bmatrix} c_{rr} & 2c_{r\theta} \\ c_{r\theta} & c_{\theta\varphi} + c_{\theta\theta} \end{bmatrix} \begin{Bmatrix} \alpha_r \\ \alpha_\theta \end{Bmatrix}, \tag{4}$$

in which α_i are the thermal expansion coefficients.

It is assumed here that magnetic permeability $\mu(r)$ of EGP sphere is similar to magnetic permeability of its medium (Ezzat, 1997). It is also assumed that the medium is non-ferromagnetic and non-ferroelectric with neglecting Thompson effect. So, the simple forms of Maxwell's equations of electrodynamics may be expressed as (Kraus 1984, Dai and Wang 2004)

$$\left.\begin{aligned} \vec{J} = \nabla \times \vec{h}, \quad \nabla \times \vec{e} = -\mu \frac{\partial \vec{h}}{\partial t}, \\ \nabla \cdot \vec{h} = 0, \quad \vec{e} = -\mu \left(\frac{\partial \vec{u}}{\partial t} \times \vec{H}\right), \\ \vec{h} = \nabla \times (\vec{u} \times \vec{H}). \end{aligned}\right\} \tag{5}$$

The vector of initial magnetic $\vec{H} \equiv (0,0,H_\varphi)$ and displacement field $\vec{u} \equiv (u,0,0)$ as well as $\vec{h} \equiv (0,0,h_\varphi)$ may be applied in Eq. (5), to get

$$\vec{e} \equiv -\mu(r)\left(0, H_\varphi \frac{\partial u}{\partial t}, 0\right),$$
$$\vec{J} \equiv \left(0, -\frac{\partial h_\varphi}{\partial r}, 0\right),$$
$$h_\varphi = -H_\varphi\left(\frac{\partial u}{\partial r} + \frac{2u}{r}\right).$$
$$\tag{6}$$

Generally, this study assumes that all properties, c_{ij}, e_{rj}, ε_{rr}, μ, η_i, α_i and p_{rr}, change continuously along the radial direction of EGP sphere according to the exponentially graded relation presented in Eq. (1).

3. Governing equations

3.1 Temperature and moisture equations

The temperature distribution along the radial direction of EGP hollow sphere is given by thermal conduction equation (Allam *et al.* 2008):

$$\kappa \nabla^2 T(r) + q(r) = 0, \tag{7}$$

where $\nabla^2 = \frac{d^2}{dr^2} + \frac{1}{r}\frac{d}{dr}$, κ represents the thermal conductivity and $q(r)$ denotes the heat generation function.

The equation of transient moisture diffusion will be expressed by using Fick's law as

$$\nabla^2 C(r) = 0. \tag{8}$$

3.2 Equations of charge and equilibrium

The equilibrium equation of EGP hollow sphere, with neglecting body forces, may be written as (Dai *et al.* 2006):

$$\frac{d\sigma_r}{dr} + \frac{2(\sigma_r - \sigma_\theta)}{r} + f_\varphi = 0. \tag{9}$$

where f_φ represents Lorentz force. It is expressed as (Dai *et al.* 2006):

$$f_\varphi = H_\varphi^2 \frac{d}{dr}\left(\mu \frac{du}{dr} + 2\mu \frac{u}{r}\right). \tag{10}$$

Once again, if we neglect the free charge density, we can get the charge equation of electrostatics as (Heyliger, 1997):

$$\frac{dD_r}{dr} + \frac{2D_r}{r} = 0. \tag{11}$$
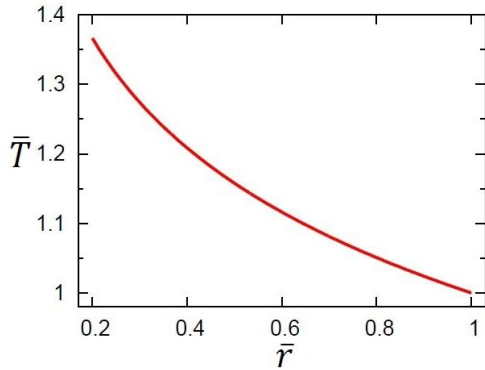
Fig. 1 Temperature distribution in EGP hollow sphere
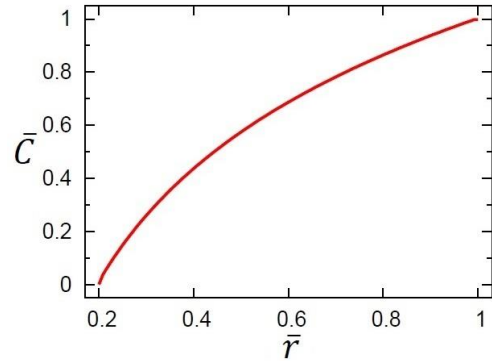
Fig. 2 Moisture distribution in EGP hollow sphere
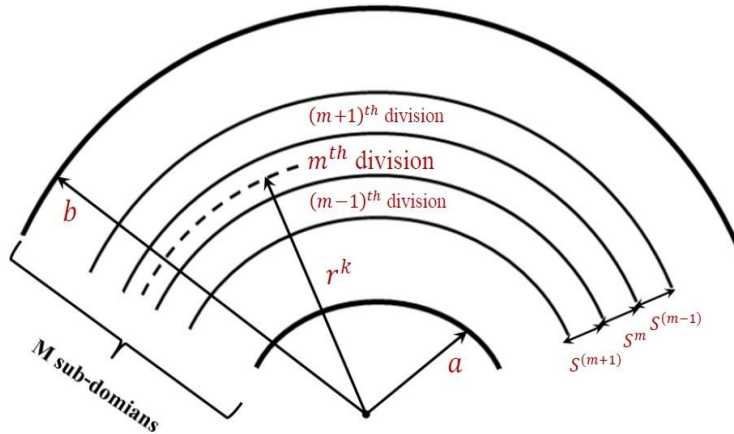
Fig. 3 Dividing radial domain into some finite sub-domain

4. Elastic solutions for EGP hollow sphere

The purpose of this section is to solve the different equations of temperature, moisture and equilibrium. All integration constants will be determined by applied boundary conditions of pressure and electric potential.

The inner surface of EGP hollow sphere is subjected to reference initial heat T_0 and its outer surface is insulated. The heat conditions for temperature are

$$T(r)|_{r=a} = T_0, \quad \left.\frac{dT(r)}{dr}\right|_{r=b} = 0. \tag{12}$$

The heat generation function is prescribed as

$$q(r) = -Q\left(\frac{r-a}{a}\right)\left(\frac{r-b}{b}\right), \quad a \leq r \leq b, \tag{13}$$

where Q denotes the uniform rate of internal energy generation. Solving Eq. (7) gives

$$T(r) = \frac{Qr^2}{144\kappa ab}[9(r^2 + 4ab) - 16r(a + b)] + c_1 \ln(r) + c_2, \tag{14}$$

where c_1 and c_2 are integration constants which derived with the help of Eq. (12). That is

$$\left. \begin{aligned} c_1 &= \frac{Qb^2}{12\kappa a}(b - 2a), \\ c_2 &= \frac{Q}{144\kappa ab}[a^3(7a - 20b) - 12b^3 \ln(a)(b - 2a)] + T_0. \end{aligned} \right\} \tag{15}$$

Figure 1 illustrates the behavior of non-dimensional temperature $\bar{T} = T/T_0$ along radial direction with $\bar{r} = r/b$. The two radii of EGP hollow sphere are fixed as $a = 0.2$ m and $b = 1$ m. Also, Q and κ are presented as

$$Q = 12 \ (\text{W/m}^3), \quad \kappa = 0.35 \ (\text{W/K m}). \tag{16}$$

The moisture concentration at boundaries are represented as

$$C(r)|_{r=a} = 0, \qquad C(r)|_{r=b} = C_0, \tag{17}$$

where C_0 denotes reference initial moisture concentration. Now, solving Eq. (8) gives

$$C(r) = c_3 \ln(r) + c_4, \tag{18}$$

in which c_3 and c_4 are additional integration constants. They are, due to Eqs. (17), given by

$$c_3 = \frac{C_0}{\ln(b) - \ln(a)}, \qquad c_4 = -\frac{C_0 \ln(a)}{\ln(b) - \ln(a)}. \tag{19}$$

Figure 2 plots the distribution of non-dimensional moisture concentration $\bar{C} = C/C_0$ through the radial direction with $\bar{r} = r/b$.

Now, solving the charge equation of electrostatics yields

$$D_r = \frac{A_1}{r^2}, \tag{20}$$

where A_1 is integration parameter. Then, Eqs. (3) and (20) after using the gradation relation appeared in Eq. (1) give

$$\frac{\mathrm{d}\psi}{\mathrm{d}r} = \frac{1}{\varepsilon_{rr}}\left(e_{rr}\frac{\mathrm{d}u}{\mathrm{d}r} + 2e_{r\theta}\frac{u}{r} + p_{11}T - \frac{A_1}{r^2}\right) \tag{21}$$

The radial and hoop stresses appeared in Eq. (2) with the help of Eqs. (1) and (21) may be simplified by

$$\begin{Bmatrix} \sigma_r \\ \sigma_\theta \end{Bmatrix} = \left(\begin{bmatrix} m_{11} & 2m_{12} \\ m_{12} & m_{22} \end{bmatrix} \begin{Bmatrix} \frac{\mathrm{d}u}{\mathrm{d}r} \\ \frac{u}{r} \end{Bmatrix} + \begin{Bmatrix} m_{31} \\ m_{32} \end{Bmatrix} T(r) + \begin{Bmatrix} m_{41} \\ m_{42} \end{Bmatrix} C(r) \right) - \begin{Bmatrix} m_{51} \\ m_{52} \end{Bmatrix} \frac{A_1}{r^2}, \tag{22}$$

where m_{ij} are functions of r

$$m_{11} = c_{rr} + \frac{(e_{rr})^2}{\epsilon_{rr}}, \quad m_{12} = c_{r\theta} + \frac{e_{rr}e_{r\theta}}{\epsilon_{rr}}, \quad m_{22} = c_{\theta\varphi} + c_{\theta\theta} + 2\frac{(e_{r\theta})^2}{\epsilon_{rr}},$$

$$m_{31} = \frac{e_{rr}p_{11}}{\epsilon_{rr}} - \lambda_r, \quad m_{32} = \frac{e_{r\theta}p_{11}}{\epsilon_{rr}} - \lambda_\theta, \quad m_{41} = -\eta_r, \tag{23}$$

$$m_{42} = -\eta_\theta, \quad m_{51} = \frac{e_{rr}}{\epsilon_{rr}}, \quad m_{52} = \frac{e_{r\theta}}{\epsilon_{rr}}.$$

Therefore, Eq. (9) with the help of Eq. (22) gives

$$\frac{d^2u}{dr^2} + \left(\frac{\frac{dm_{11}}{dr} + H_\varphi^2 \frac{d\mu}{dr}}{m_{11} + \mu H_\varphi^2} + \frac{2}{r}\right)\frac{du}{dr} + 2\left(\frac{\frac{dm_{12}}{dr} + H_\varphi^2 \frac{d\mu}{dr}}{r(m_{11} + \mu H_\varphi^2)} + \frac{m_{12} - m_{22} - \mu H_\varphi^2}{r^2(m_{11} + \mu H_\varphi^2)}\right)u + \frac{m_{41}}{m_{11} + \mu H_\varphi^2}\frac{dC}{dr}$$

$$+ \left(\frac{\frac{dm_{41}}{dr}}{m_{11} + \mu H_\varphi^2} + \frac{2(m_{41} - m_{42})}{r(m_{11} + \mu H_\varphi^2)}\right)C(r) + \frac{m_{31}}{(m_{11} + \mu H_\varphi^2)}\frac{dT}{dr} + \left(\frac{\frac{dm_{31}}{dr}}{m_{11} + \mu H_\varphi^2} + \frac{2(m_{31} - m_{32})}{r(m_{11} + \mu H_\varphi^2)}\right)T(r) \tag{24}$$

$$- \left(\frac{\frac{dm_{51}}{dr}}{r^2(m_{11} + \mu H_\varphi^2)} - \frac{2m_{52}}{r^3(m_{11} + \mu H_\varphi^2)}\right)A_1 = 0$$

The conditions of EGP hollow sphere at its boundaries are represented as

$$\sigma_r|_{r=a} = -P_1, \qquad \sigma_r|_{r=b} = -P_2. \tag{25}$$

where P_1 and P_2 are the inner and outer pressures. Now, solving Eq. (24) to obtain the radial displacement u and using it to get the electric potential. The integration of Eq. (20) yields $\psi(r)$ with integration constant A_2. Now, the two constants A_1 and A_2 will be obtained after applying the electric conditions:

$$\psi(r)|_{r=a} = \psi_1, \qquad \psi(r)|_{r=b} = \psi_2. \tag{26}$$

Now, it is difficult to get the analytical solution of the second-order differential equation of variable coefficients appeared in Eq. (24). A semi-analytical method is presented here for this purpose. In this approach, radial domain is divided into some virtual sub-domains of thickness $s^{(k)}$ as illustrated in Figure 3. Let $r = r^{(k)}$ is said to be the mean radius of the kth division. That is

$$\frac{d^2u^{(k)}}{dr^2} + N_1^{(k)}\frac{du^{(k)}}{dr} + N_2^{(k)}u^{(k)} - N_3^{(k)} = 0, \tag{27}$$

where

$$N_1^{(k)} = \frac{\left(\frac{dm_{11}}{dr} + H_\varphi^2 \frac{d\mu}{dr}\right)\Big|_{r=r^{(k)}}}{m_{11}r^{(k)} + \mu r^{(k)}H_\varphi^2} + \frac{2}{r^{(k)}}, \tag{28}$$

$$N_2^{(k)} = \frac{2\left(\frac{\mathrm{d}m_{12}}{\mathrm{d}r}+H_\varphi^2\frac{\mathrm{d}\mu}{\mathrm{d}r}\right)\big|_{r=r^{(k)}}}{r^{(k)}\left(m_{11}r^{(k)}+\mu r^{(k)}H_\varphi^2\right)} + \frac{2\left(m_{12}r^{(k)}-m_{22}r^{(k)}-\mu r^{(k)}H_\varphi^2\right)}{\left(r^{(k)}\right)^2\left(m_{11}r^{(k)}+\mu r^{(k)}H_\varphi^2\right)},$$

$$N_3^{(k)} = \frac{m_{41}r^{(k)}}{m_{11}r^{(k)}+\mu r^{(k)}H_\varphi^2}\frac{\mathrm{d}C}{\mathrm{d}r}\bigg|_{r=r^{(k)}} + \left(\frac{\frac{\mathrm{d}m_{41}}{\mathrm{d}r}\big|_{r=r^{(k)}}}{m_{11}r^{(k)}+\mu r^{(k)}H_\varphi^2} + \frac{2\left(m_{41}r^{(k)}-m_{42}r^{(k)}\right)}{r^{(k)}\left(m_{11}r^{(k)}+\mu r^{(k)}H_\varphi^2\right)}\right)C$$

$$+\frac{m_{31}r^{(k)}}{m_{11}r^{(k)}+\mu r^{(k)}H_\varphi^2}\frac{\mathrm{d}T}{\mathrm{d}r}\bigg|_{r=r^{(k)}} + \left(\frac{\frac{\mathrm{d}m_{31}}{\mathrm{d}r}\big|_{r=r^{(k)}}}{m_{11}r^{(k)}+\mu r^{(k)}H_\varphi^2} + \frac{2\left(m_{31}r^{(k)}-m_{32}r^{(k)}\right)}{r^{(k)}\left(m_{11}r^{(k)}+\mu r^{(k)}H_\varphi^2\right)}\right)T$$

$$-\left(\frac{\frac{\mathrm{d}m_{51}}{\mathrm{d}r}\big|_{r=r^{(k)}}}{\left(r^{(k)}\right)^2\left(m_{11}r^{(k)}+\mu r^{(k)}H_\varphi^2\right)} - \frac{2m_{52}r^{(k)}}{\left(r^{(k)}\right)^3\left(m_{11}r^{(k)}+\mu r^{(k)}H_\varphi^2\right)}\right)A_1$$

The above technique is used in Eq. (24) to change it into a system of m equations where m represents the number of virtual sub-domains. Now, the solution of Eq. (27) may be expressed as

$$u^{(k)} = B_1^{(k)}\mathrm{e}^{\beta_1 r} + B_2^{(k)}\mathrm{e}^{\beta_2 r} + \frac{N_3^{(k)}}{N_2^{(k)}}, \tag{29}$$

where β_1 and β_2 are the roots of $\beta^2 + N_1^{(k)}\beta + N_2^{(k)} = 0$, and $B_1^{(k)}$ and $B_2^{(k)}$ are unknown parameters for the kth sub-domain. This solution is valid only for

$$r^{(k)} - \frac{s^{(k)}}{2} \le r \le r^{(k)} + \frac{s^{(k)}}{2}, \tag{30}$$

in which $r^{(k)}$ and $s^{(k)}$ represent mean radius and radial width of kth sub-domain, respectively. The unknown parameters $B_1^{(k)}$ and $B_2^{(k)}$ may be derived by applying sub-domain conditions. The continuity of all variables is imposed on the interfaces of adjacent sub-domains. That is

$$\begin{aligned} u^{(k)}\left(r^{(k)}+\frac{S^{(k)}}{2}\right) &= u^{(k+1)}\left(r^{(k+1)}-\frac{S^{(k+1)}}{2}\right), \\ \sigma_r^{(k)}\left(r^{(k)}+\frac{S^{(k)}}{2}\right) &= \sigma_r^{(k+1)}\left(r^{(k+1)}-\frac{S^{(k+1)}}{2}\right), \\ \sigma_\theta^{(k)}\left(r^{(k)}+\frac{S^{(k)}}{2}\right) &= \sigma_\theta^{(k+1)}\left(r^{(k+1)}-\frac{S^{(k+1)}}{2}\right), \\ \psi^{(k)}\left(r^{(k)}+\frac{S^{(k)}}{2}\right) &= \psi^{(k+1)}\left(r^{(k+1)}-\frac{S^{(k+1)}}{2}\right). \end{aligned} \tag{31}$$

The above conditions together with Eqs. (25) and (26) yield a set of linear algebraic equations in $A_{1,k}$, $A_{2,k}$, $B_{1,k}$, $B_{2,k}$ ($k = 1,2,...,m$). Solving these equations and using them in Eqs. (29), the displacements $u^{(k)}$ will be obtained in each sub-domain. The accuracy of the results is improved as the number of divisions increases.

5. Numerical examples and discussions

This section is concerned with the numerical examples for analyses of EGP hollow spheres in hygrothermal environment. Numerical computations will be carried out for different fields with $H_\varphi = 2.23\,\text{GA/m}$. The dimensionless of radial displacement is $\bar{u} = 10^2 u/b$ while the dimensionless of stresses and electric potential will be given according the case studied.

The material properties of the inner surface of EGP hollow sphere are assumed as (Dai *et al.* 2010):

$$c_{rr}^a = 1.11 \times 10^{11}\,\text{Pa}, \quad c_{r\theta}^a = 7.78 \times 10^{10}\,\text{Pa}, \quad c_{\theta z}^a = 1.15 \times 10^{11}\,\text{Pa},$$

$$c_{\theta\theta}^a = 2.2 \times 10^{11}\,\text{Pa}, \quad e_{rr}^a = 15.1\,\text{C/m}^2, \quad e_{r\theta}^a = -5.2\,\text{C/m}^2,$$

$$\varepsilon_{rr}^a = 5.62 \times 10^{-9}\,\text{C}^2/\text{K\,m}^2, \quad p_{11}^a = -2.5 \times 10^{-5}\,\text{C/km}^2, \tag{32}$$

$$\alpha_r^a = 0.0001\,\text{K}^{-1}, \quad \alpha_\theta^a = 0.00001\,\text{K}^{-1},$$

$$\eta_r^a = 0.03 \times c_{rr}^a, \quad \eta_\theta^a = 0.02 \times c_{rr}^a.$$

Also, material properties of outer surface of EGP hollow sphere are assumed with references to PZT-5 as (Ghorbanpour Arani *et al.* 2011):

$$c_{rr}^b = 1.11 \times 10^{11}\,\text{Pa}, \quad c_{r\theta}^b = 7.52 \times 10^{10}\,\text{Pa}, \quad c_{\theta z}^b = 7.8 \times 10^{10}\,\text{Pa},$$

$$c_{\theta\theta}^b = 1.2 \times 10^{11}\,\text{Pa}, \quad e_{rr}^b = 15.78\,\text{C/m}^2, \quad e_{r\theta}^b = -5.35\,\text{C/m}^2,$$

$$\varepsilon_{rr}^b = 7.4 \times 10^{-9}\,\text{C}^2/\text{K\,m}^2, \quad p_{11}^b = -2.94 \times 10^{-5}\,\text{C/km}^2, \tag{33}$$

$$\alpha_r^b = 8.53 \times 10^{-6}\,\text{K}^{-1}, \quad \alpha_\theta^b = 1.99 \times 10^{-6}\,\text{K}^{-1},$$

$$\eta_r^b = 0.01 \times c_{rr}^b, \quad \eta_\theta^b = 0.02 \times c_{rr}^b.$$

5.1 Example 1

This example show that the outer surface of EGP sphere is subjected to constant pressure while its inner surface is traction free. Also, the outer surface is under uniform potential and its inner one is grounded. So, it is assumed that

$$P_1 = 0, \quad P_2 = 10^{10}\,\text{Pa}, \quad \psi_1 = 0, \quad \psi_2 = 10^8\,\text{W/A} \tag{34}$$

The results in this example are illustrated in Figures 4-7. The dimensionless stresses and electric potential are expressed as

$$\bar{\sigma}_i = \frac{\sigma_i}{P_2}, \quad \bar{\psi} = \frac{\psi}{\psi_2}. \tag{35}$$

Figure 4 shows the radial displacement $\bar{u}$ is decreasing along the radial direction. The radial displacement $\bar{u}$ of material 2 is maximum at the inner surface and minimum at the outer one while $\bar{u}$ of material 1 is minimum at inner surface and maximum at outer one. Figure 5 shows
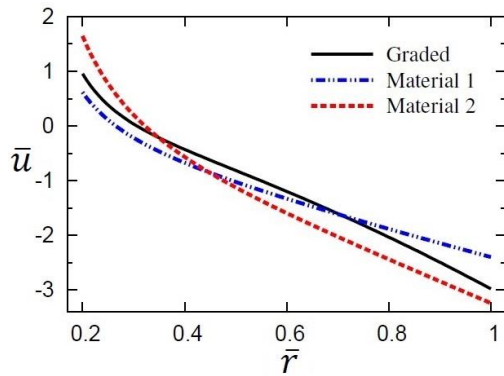
Fig. 4 Radial displacement in EGP hollow sphere
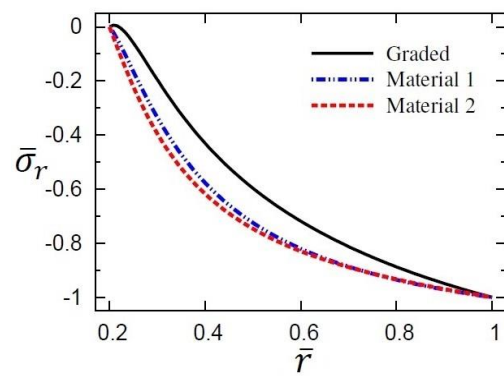
Fig. 5 Radial stress distribution in EGP hollow sphere
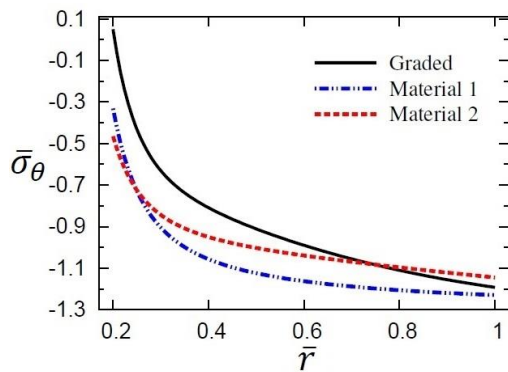
Fig. 6 Hoop stress distribution in EGP hollow sphere
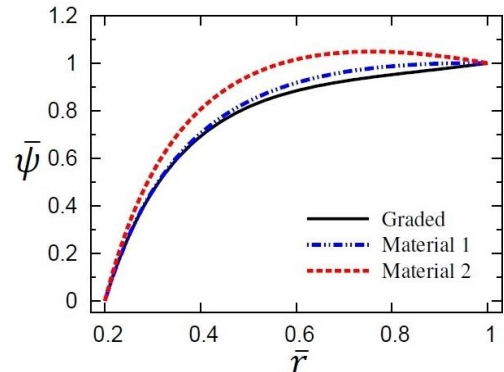
Fig. 7 Electric potential distribution in EGP hollow sphere

that $\bar{\sigma}_r$ vanishes at inner surface and $\bar{\sigma}_r = -1$ at $\bar{r} = 1$, which satisfies its boundary conditions. It is clear that the value of $\bar{\sigma}_r$ of graded sphere is the greatest one comparing to those of homogenous materials. Figure 6 shows that $\bar{\sigma}_\theta$ is decreasing along the radial direction. The graded sphere gives the maximum hoop stress $\bar{\sigma}_\theta$ at its inner surface. Also, the homogeneous sphere of material 1 gives the minimum hoop stress $\bar{\sigma}_\theta$ at the outer surface. Figure 7 shows that the electric potentials $\bar{\psi}$ of graded sphere and homogeneous sphere of material 1 are increasing along the radial direction of EGP sphere. The electric potential $\bar{\psi}$ of homogeneous sphere of material 2 is no longer increasing and has its absolute maximum near outer surface of EGP sphere. Also, $\bar{\psi}$ satisfies the boundary conditions that given in Eq. (33).

5.2 Example 2

The inner surface of EGP sphere is under constant pressure and sphere is free of electric potential. In this case, the sphere acts as a sensor with

$$P_1 = 10^{10} \text{ Pa}, \quad P_2 = 0, \quad \psi_1 = \psi_2 = 0. \tag{36}$$
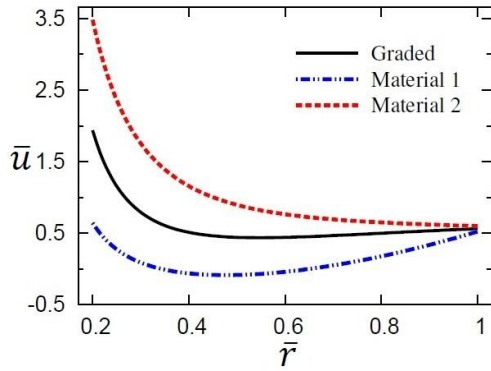
Fig. 8 Radial displacement in EGP hollow sphere
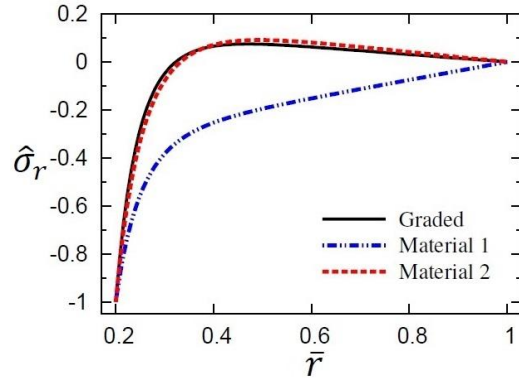
Fig. 9 Radial stress distribution in EGP hollow sphere
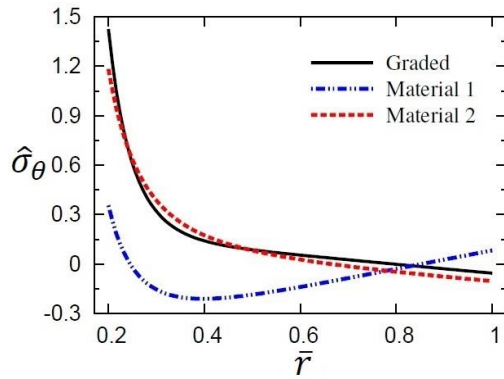
Fig. 10 Hoop stress distribution in EGP hollow sphere
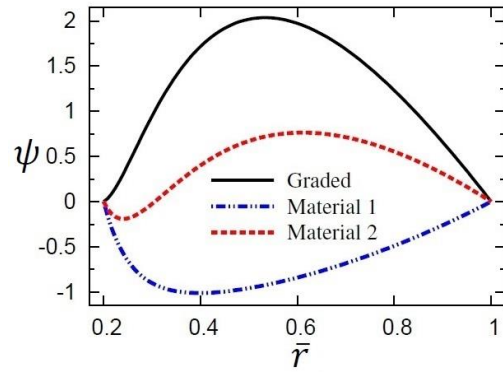
Fig. 11 Electric potential distribution in EGP hollow sphere

The results of this example are plotted in Figures 8-11. The dimensionless stresses are given by

$$\hat{\sigma}_i = \frac{\sigma_i}{P_1} \tag{37}$$

Figures 8-11 show the distributions of all fields of the EGP hollow sphere. Figure 8 shows that the radial displacements $\bar{u}$ of the graded sphere and homogeneous sphere of material 1 are no longer decreasing and has its absolute minimum at $\bar{r} = 0.48$. However, the radial displacement $\bar{u}$ of the homogeneous sphere of material 2 is directly decreasing along the radial direction. Figure 9 shows that $\hat{\sigma}_r$ satisfies the boundary conditions. The variations between radial stresses $\hat{\sigma}_r$ increase in the neighborhood of $\bar{r} = 0.4$ in which the absolute maximum value of $\hat{\sigma}_r$ occurs for the graded sphere and the homogeneous sphere of material 2. Figure 10 shows that $\hat{\sigma}_\theta$ is decreasing to get its absolute minimum at outer surface of graded sphere and sphere of material 2. While hoop stress $\hat{\sigma}_\theta$ of sphere of material 1 is no longer decreasing and has its absolute minimum at $\bar{r} = 0.4$. It increases again to be the maximum one at the outer surface. Figure 11 shows that ψ vanishes at inner and outer surfaces according to boundary conditions. The absolute maximum values of the electric potential ψ of graded sphere and homogeneous sphere of
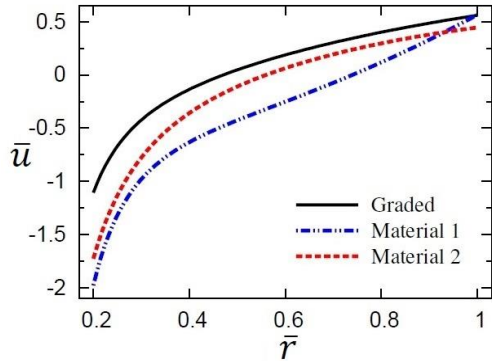
Fig. 12 Radial displacement in EGP hollow sphere
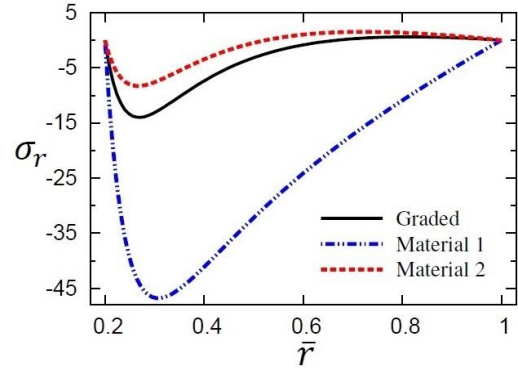
Fig. 13 Radial stress distribution in EGP hollow sphere
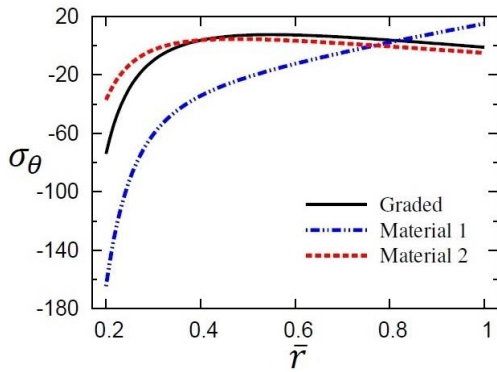
Fig. 14 Hoop stress distribution in EGP hollow sphere
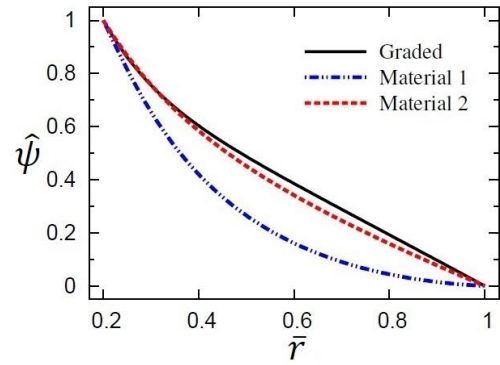
Fig. 15 Electric potential distribution in EGP hollow sphere

material 2 occur at different positions. The electric potential ψ of sphere of material 1 is no longer decreasing and has its absolute minimum at $\bar{r} = 0.4$.

5.3 Example 3

The sphere is traction free and its inner surface is under a constant voltage and it is grounded at the outer surface. That is

$$P_1 = P_2 = 0, \quad \psi_1 = 10^8 \text{ W/A}, \quad \psi_2 = 0. \tag{38}$$

Figures 12-15 show the plots of the radial displacement $\bar{u}$, radial stress σ_r, hoop stress σ_θ, and dimensionless electric potential $\hat{\psi} = \psi/\psi_1$ vs the radial direction of sphere. Figure 12 shows that $\bar{u}$ is increasing along the radial direction to reach its maximum at the outer surface. The radial displacements of graded sphere are the greatest ones. Figure 13 shows that σ_r satisfies the boundary conditions it vanishes at the sphere boundaries. The minimum values of σ_r occur at the interval $0.25 \leq \bar{r} \leq 0.33$. Figure 14 displays the hoop stress σ_θ which increases to its absolute maximum at the outer surface of homogeneous sphere of material 1. This is not the same for other spheres. Figure 15 shows that $\hat{\psi}$ vanishes at the outer surface and is equal to 1 at $\bar{r} = 0.2$. The
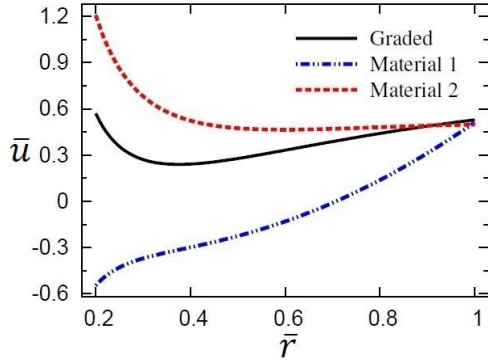
Fig. 16 Radial displacement in EGP hollow sphere
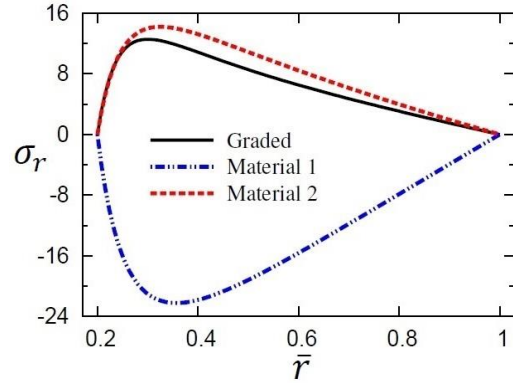
Fig. 17 Radial stress distribution in EGP hollow sphere
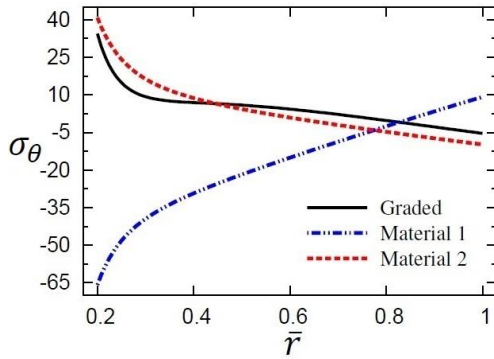
Fig. 18 Hoop stress distribution in EGP hollow sphere
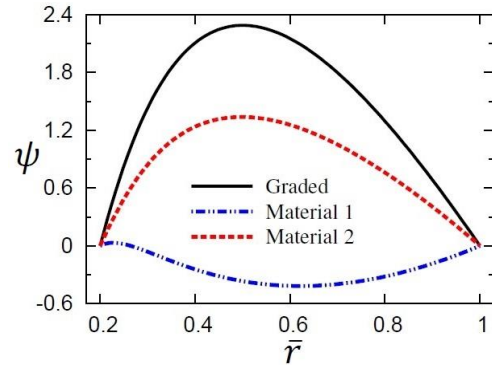
Fig. 19 Electric potential distribution in EGP hollow sphere

variations between electric potentials $\hat{\psi}$ decrease at $\bar{r} = 0.6$.

5.4 Example 4

The sphere is traction free and insulated, that is:

$$P_1 = P_2 = 0, \quad \psi_1 = \psi_2 = 0. \tag{39}$$

Figures 16-19 show the radial displacement, radial stress, hoop stress and electric potential distributions in sphere, respectively. Figure 16 shows that $\bar{u}$ is increasing to get its absolute maximum at outer surface of the homogeneous sphere of material 1. However, $\bar{u}$ decreases to its absolute minimum at outer surface of homogeneous sphere of material 2. Finally, $\bar{u}$ of the graded sphere is no longer decreasing and has its absolute minimum at $\bar{r} = 0.38$. Figure 17 shows that σ_r satisfies the conditions at the sphere boundaries. The absolute maximum of σ_r occurs at $0.30 \leq \bar{r} \leq 0.35$ for homogeneous sphere of material 2 and graded sphere. Also, absolute minimum of σ_r occurs at $\bar{r} = 0.35$ for homogeneous sphere of material 1. Also, Figure 18 shows that σ_θ of homogeneous sphere of material 1 is increasing along the radial directions while those of graded material and homogeneous sphere of material 2 are decreasing. Figure 19 shows

that ψ vanishes at $\bar{r} = 0.2$ and $\bar{r} = 1$ as given in Eq. (39). The absolute maximum value of ψ occurs at $\bar{r} = 0.5$ for graded sphere and homogeneous sphere of material 2. Also, The absolute minimum value of ψ occurs at $\bar{r} = 0.6$ for homogeneous sphere of material 1.

6. Conclusions

• This article presented the hygrothermal analyses of functionally graded piezoelectric hollow sphere.

• A semi-analytical technique is improved to deduce all fields in which the radial stress and electric potential are assumed to be under combined mechanical and electrical loadings.

• Four examples are discussed to illustrate different types of hollow spheres. First, the outer surface of EGP sphere is subjected to constant pressure under uniform potential while its inner surface is traction free and grounded. Second, the inner surface is under constant pressure and sphere is free of electric potential. Third, the sphere is traction free and its inner surface is under a constant voltage while its outer surface is grounded. Finally, the sphere is traction free and insulated.

• From the results, it is clear that the gradation plays an important role to control the distribution of all fields. Thus, the selection of a proper value of graded index n, a suitable radial pressure and electric potential make it is possible for engineers to design the EGP hollow sphere that can meet other special requirements.

• It is concluded that the semi-analytical solution is an accurate and reliable and this method is simple and effective.

References

Akavci, S.S. and Tanrikulu, A.H. (2008), "Buckling and free vibration analyses of laminated composite plates by using two new hyperbolic shear-deformation theories", *Mech. Compos. Mater.*, **44**(2), 145-154.

Akbarzadeh, A.H and Chen, Z.T. (2013), "Hygrothermal stress in one-dimensional functionally graded piezoelectric media in constant magnetic field", *Compos. Struct.*, **97**, 317-331.

Allam, M.N.M. and Tantawy, R. (2011), "Thermomagnetic viscoelastic responses in functionally graded hollow structures", *Acta Mech. Sinica*, **27**(4), 567-577.

Allam, M.N.M., Tantawy, R. and Zenkour, A.M. (2015), "Semi-empirical and efficient solutions for FGPM hollow spheres in hygrothermal environment", *KSCE J. Civil Eng.*, **20**(5), 1-8.

Allam, M.N.M., Tantawy, R., Yousof, A. and Zenkour, A.M. (2017), "Elastic and viscoelastic stresses of nonlinear rotating functionally graded solid and annular disks with gradually varying thickness", *Arch. Mech. Eng.*, **4**, 423-440.

Allam, M.N.M., Zenkour, A.M. and Tantawy, R. (2014), "Analysis of functionally graded piezoelectric cylinders in a hygrothermal environment", *Adv. Appl. Math. Mech.*, **6**(2), 233-246.

Arani, A.G., Kolahchi, R. and Barzoki, A.M. (2011), "Effect of material in-homogeneity on electro-thermo-mechanical behaviors of functionally graded piezoelectric rotating shaft", *Appl. Math. Model.*, **35**, 2771-2789.

Arani, A.G., Kolahchi, R., Barzoki, A.M. and Loghman, A. (2012), "Electro-thermo-mechanical behaviors of FGPM spheres using analytical method and ANSYS software", *Appl. Math. Model.*, **36**, 139-157.

Arani, A.G., Salari, M., Khademizadeh, H. and Arefmanesh, A. (2009), "Magnetothermoelastic transient response of a functionally graded thick hollow sphere subjected to magnetic and thermoelastic fields", *Arch. Appl. Mech.*, **79**, 481.

Arefi, M. and Nahas, I. (2014), "Nonlinear electro thermo elastic analysis of a thick spherical functionally graded piezoelectric shell", *Compos. Struct.*, **118**, 510-518.

Bahrami, A. and Nasier, A. (2007), "Interlaminar hygrothermal stresses in laminated plates", *J. Solids Struct.*, **44**, 8119-8142.

Chen, J.Y., Pan, E. and Heyliger, P.R. (2015), "Static deformation of a spherically anisotropic and multilayered magneto-electro-elastic hollow sphere", *J. Solids Struct.*, **60-61**, 66-74.

Chiroiu, V. and Munteanu, L. (2007), "On the free vibrations of a piezoceramic hollow sphere", *Mech. Res. Commun.*, **34**, 123-129.

Dai, H.L. and Fu, Y.M. (2005), "Electromagnetotransient stress and perturbation of magnetic field vector in transversely isotropic piezoelectric solid spheres", *Mater. Sci. Eng.* B, **129**(1-3), 86-92.

Dai, H.L. and Rao, Y.N. (2011), "Investigation on electromagnetothermoelastic interaction of functionally graded piezoelectric hollow spheres", *Struct. Eng. Mech.*, **40**(1), 49-64.

Dai, H.L. and Wang, X. (2004), "Dynamic responses of piezoelectric hollow cylinders in an axial magnetic field", *J. Solid Struct.*, **41**, 5231-5246.

Dai, H.L. and Wang, X. (2005), "Thermo-electro-elastic transient responses in piezoelectric hollow structures", *J. Solids Struct.*, **42**, 1151-1171.

Dai, H.L., Fu, Y.M. and Yang, J.H. (2007), "Electromagnetoelastic behaviors of functionally graded piezoelectric solid cylinder and sphere", *Acta Mech. Sinica*, **23**, 55-63.

Dai, H.L., Fu, Y.M., Yang, J.H. and Dong, Z.M. (2006), "Exact solutions for functionally graded pressure vessels in a uniform magnetic field", *J. Solids Struct.*, **43**, 5570-5580.

Dai, H.L., Hong, L., Fu, Y.M. and Xiao, X. (2010), "Analytical solution for electromagneto thermoelastic behaviors of a functionally graded piezoelectric hollow cylinder", *Appl. Math. Model.*, **34**, 343-357.

Dai, H.L., Jiang, H.J. and Yang, L. (2012), "Time-dependent behaviors of a FGPM hollow sphere under the coupling of multi-fields", *Solid State Sci.*, **14**, 587-597.

Dai, H.L., Xiao, X. and Fu, Y.M. (2010), "Analytical solutions of stresses in functionally graded piezoelectric hollow structures", *Solid State Commun.*, **150**, 763-767.

Dai, H.L., Yang, L. and Zheng, H.Y. (2011), "Magnetothermoelastic analysis of functionally graded hollow spherical structures under thermal and mechanical loads", *Solid State Sci.*, **13**, 372-378.

Ding, H.J., Wang, H.M. and Chen, W.Q. (2003), "Dynamic responses of a functionally graded pyroelectric hollow sphere for spherically symmetric problems", *J. Mech. Sci.*, **45**, 1029-1051.

Eslami, M.R., Babaei, M.H. and Poultangari, R. (2005), "Thermal and mechanical stresses in a functionally graded thick sphere", *J. Press. Vessels Piping*, **82**, 522-527.

Ezzat, M.A. (1997), "Generation of generalized thermomagnetoelastic waves by thermal shock in a perfectly conducting half-space", *J. Therm. Stresses*, **20**, 633-917.

Guo, G., En-Bo, W. and Chen, X. (2009), "Effective elastic properties of piezoelectric composites with radially polarized cylinders", *Phys. B*, **404**, 4001-4006.

Heyliger, P. (1997), "A note on the static behavior of simply-supported laminated piezoelectric cylinders", *J. Solids Struct.*, **34**, 3781-3794.

Jabbari, M, Karampour, S. and Eslami, M.R. (2013), "Steady state thermal and mechanical stresses of a poro-pizo-FGM hollow sphere", *Mecc.*, **48**, 699-719.

Kar, A. and Kanoria, M. (2009), "Generalized thermoelastic functionally graded orthotropic hollow sphere under thermal shock with three-phase-lag effect", *Europ. J. Mech. A/Solids*, **28**, 757-767.

Kraus, J.D. (1984), *Electromagnetic*, McGraw Hill, Inc., U.S.A.

Lo, S.H., Zhen, W.U., Cheung, Y.K. and Wanji, C. (2010), "Hygrothermal effects on multilayered composite plates using a refined higher order theory", *Compos. Struct.*, **92**, 633-646.

Loghman, A., Ghorbanpour Arani, A. and Aleayoub, S.M.A. (2011), "Time-dependent creep stress redistribution analysis of thick-walled functionally graded spheres", *Mech. Time-Dependent Mater.*, **15**(4), 353-365.

Ootao, Y. and Ishihara, M. (2012), "Exact solution of transient thermal stress problem of a multilayered magneto-electro-thermoelastic hollow sphere", *Appl. Math. Model.*, **36**(4), 1431-1443.

Ootao, Y. and Tanigawa, Y. (2007), "Transient piezothermoelastic analysis for a functionally graded

thermopiezoelectric hollow sphere", *Compos. Struct.*, **81**(4), 540-549.

Patel, B.P., GanaPathi, M. and Makhecha, D.P. (2002), "Hygrothermal effect on the structural behavior of thick composite laminates using higher-order theory", *Compos. Struct.*, **56**(1), 25-34.

Poultangari, R., Jabbari, M. and Eslami, M.R. (2008), "Functionally graded hollow spheres under non-axisymmetric thermo-mechanical loads", *J. Press. Vessels Piping*, **85**(5), 295-305.

Raja, S., Sinha, P.K., Prathap, G. and Dwarakanathan, D. (2004), "Influence of active stiffening on dynamic behavior of piezo-hygro-thermo elastic composite plates and shell", *J. Sound Vib.*, **278**, 257-283.

Reddy, J.N. (2000), "Analysis of functionally graded plates", *J. Numer. Meth. Eng.*, **47**, 663-684.

Reddy, J.N. and Cheng, Z.Q. (2001), "Three-dimensional thermomechanical deformations of functionally graded rectangular plates", *Europ. J. Mech. A/Solids*, **20**(5), 841-855.

Reddy, J.N. and Chin, C.D. (1998), "Thermomechanical analysis of functionally graded cylinders and plates", *J. Therm. Stresses*, **21**(6), 593-626.

Sinha, D.K. (1962), "Note on the radial deformation of a piezoelectric polarized spherical shell with symmetrical temperature distribution", *J. Acoust. Soc. Amer.*, **34**(8), 1073-1075.

Wang, H.M. and Ding, H.J. (2006), "Transient responses of a magneto-electro-elastic hollow sphere for fully coupled spherically symmetric problem", *Europ. J. Mech. A/Solids*, **25**, 965-980.

Wang, H.M. and Xu, Z.X. (2010), "Effect of material inhomogeneity on electromechanical behaviors of functionally graded piezoelectric spherical structures", *Comput. Mater. Sci.*, **48**(2), 440-445.

Whiteny, J.M. and Ashton, J.E. (1971), "Effect of environment on the elastic response of layered composite plates", *AIAA J.*, **9**(9), 1708-1713.

Zenkour, A.M. (2005a) "A comprehensive analysis of functionally graded sandwich plates: Part 1 Deflection and stresses", *Int. J. Solids Struct.*, **42**(18-19), 5224-5242.

Zenkour, A.M. (2005b), "A comprehensive analysis of functionally graded sandwich plates: Part 2 Buckling and free vibration", *Int. J. Solids Struct.*, **42**(18-19), 5243-5258.

Zenkour, A.M. (2006), "Generalized shear deformation theory for bending analysis of functionally graded plates", *Appl. Math. Model.*, **30**(1), 67-84.

Zenkour, A.M. (2007), "Benchmark trigonometric and 3-D elasticity solutions for an exponentially graded thick rectangular plate", *Arch. Appl. Mech.*, **77**(4), 197-214.

Zenkour, A.M., Elsibai, K.A. and Mashat, D.S. (2008), "Elastic and viscoelastic solutions to rotating functionally graded hollow and solid cylinders", *Appl. Math. Mech.*, **29**(12), 1601-1616.

TK